Rotational bands in the baryon spectrum. II

M. V. N. Murthy, Mira Dey,* Jishnu Dey,* and R. K. Bhaduri
Physics Department, McMaster University, Hamilton, Ontario, Canada L8S 4M1
(Received 16 December 1983; revised manuscript received 12 March 1984)

A nonrelativistic constituent quark model is developed for baryons where the quarks are moving in a deformable mean field. The deformation parameters in each state are determined by minimization of the energy, subject to the constraint of volume conservation in the state. It is found that while the ground state is spherical, the excited-state configurations are deformed. The deformation increases with excitation energy. This is responsible for the observed low-lying states $N(1440)\frac{1}{2}^+$ and $\Delta(1900)\frac{1}{2}^-$. The experimental states are grouped in rotational bands, and the deduced moment-of-inertia parameter is shown to be consistent with the quantum-mechanical calculation. A detailed comparison with experimental data is made.

I. INTRODUCTION

In an earlier paper[1] (hereafter referred to as I), it was proposed that many of the observed features of the excited-states spectra in the nucleon and the Δ could be qualitatively explained if it is assumed that baryons, spherical in the ground state, acquire deformation in excited states. It was pointed out that this phenomenon is not uncommon in nuclei, where sometimes rotational bands are found built on an excited-state configuration, and not on the ground state which remains very nearly spherical. Two of the striking features of the nucleon-Δ spectra are the occurrence of low-lying even-parity excitations [such as the Roper resonance $(1440)\frac{1}{2}^+$] around the same energy as the lowest odd-parity states, and also the observed low-lying set of odd-parity states around 1900 MeV in the Δ, which should have come at a much higher energy in the spherical model. We shall demonstrate in this paper that these and other aspects of the spectra can be quantitatively reproduced assuming a simple nonrelativistic constituent-quark model. In the ground state, the quarks occupy the lowest orbitals of a mean field. Excited-state configurations are obtained, as usual, by letting one or more quarks occupy higher orbitals. The new feature of our model is that the mean field for a given occupancy of orbitals is given the freedom to deform to minimize the energy of the state. In a given state, the mean field is allowed to deform only under the constraint that the volume is conserved. It is then shown that whereas in the ground state the mean field is spherical, a shape transition takes place for excited-state configurations, with the field getting more and more deformed with increasing excitation energy. This has the desirable result of explaining the spectroscopy of the baryons with a very few parameters. Before proceeding with a detailed description of the model, we shall discuss the two main ingredients in the model—the onset of deformation with excitation energy, and the concept of volume conservation.

In the MIT bag model,[2] the nonlinear boundary conditions can be satisfied for a spherical bag in the $s_{1/2}$ orbital and in the first excited $p_{1/2}$ orbital, but the bag has to deform for excited orbitals of higher angular momenta. This is because the pressure exerted by the quarks in these orbitals on the bag boundary is nonisotropic. This has inspired several authors to examine the single-particle states in a deformed bag.[3] In the constituent quark model, we take the point of view that the mean field is generated in a self-consistent manner through two- and many-body forces between the quarks. In excited-state configurations, the single-particle density of the quarks is nonisotropic, and this nonisotropy in turn reflects on the mean field in a self-consistent Hartree-type calculation. The deformation of the shape is a result of the anharmonic as well as the noncentral nature of the interquark interaction.

The next point is that of volume conservation.[4] It does *not* mean that the volume of the baryon does not increase in excited states. What it implies is that for a given configuration of orbitals in the mean field, the shape is allowed to deform without changing the volume in that state. This is a highly successful prescription in nuclear physics, where it is known that nuclear matter is highly incompressible.[5] For baryons, we have calculated the compression modulus recently, taking semirealistic quark-quark interactions.[6] It was found that baryonic matter is more than five times incompressible than nuclear matter. One way of simulating this effect of interquark forces in a mean-field calculation is to preserve volume conservation in a given state when the shape is allowed to deform. As we shall see, this has also the desirable effect that on minimization of the energy, the shape of the density follows the shape of the mean field. In our model, the volume of the baryon grows with the excitation energy, the relationship being the same as in the spherical oscillator model.

For simplicity of calculation and elimination of center-of-mass motion, we assume the mean field to be a triaxial oscillator. Upon minimization of the energy with volume conservation, it will be shown that in the ground state (with oscillator quanta $N=0$) this field is isotropic, whereas for $N=1,2$ and the lowest $N=3$ excited states, the potential shape is deformed with an axis of symmetry.

In such a potential, the single-particle orbital angular momentum l^2 is no longer a good quantum number, but its projection along the body-fixed symmetry axis, l_z, is a conserved quantity. We construct an intrinsic state by assigning the quarks in appropriate orbitals, and taking a product of the deformed single-particle orbitals. These intrinsic states are not eigenstates of total L^2. It is again known[7] from nuclear physics that projection onto states of good angular momenta from a deformed intrinsic state generates the characteristic rotational spectrum. These states have total angular momentum $L=0$, 2, 4, etc., for even-parity (prolate) states, and $L=1$, 3, 5, etc., for odd-parity excitations, which couple to the intrinsic spin $S=\frac{1}{2}$ or $S=\frac{3}{2}$ to yield states of good J.

The single-particle wave functions are determined analytically from the mean field. The model Hamiltonian also contains a spin-spin hyperfine interaction of zero range, and a residual central interaction U. The latter is taken only to first order in diagonal matrix elements, as in spherical calculations of Isgur and Karl[8] and Forsyth and Cutkosky.[9] Diagonalization of the hyperfine interaction causes mixing between the various intrinsic states. The parameters of the model are (a) the constituent quark mass (same for u and d)$=330$ MeV, (b) the single oscillator parameter b (defined in Sec. II)$=0.463$ fm, (c) the strong coupling constant $\alpha_s=0.92$, which yields the right N-Δ splitting with our choice of b, and (d) the residual interaction U, whose diagonal matrix element in the ground state is taken to be -220 MeV; in other states the matrix elements can be computed from the wave functions.

It is to be noted that the parameters (a), (b), and (c) are about the same as those used by Isgur and Karl[8] in their calculation with the spherical model. Our parameter (d) is of about half their strength, presumably because deformation of the mean field is already accounting for much of the anharmonicity. In spherical calculations, Forsyth and Cutkosky[9] have carefully examined the $N=3$ odd-parity states, and they require an additional parameter in the symmetric states to bring them down in energy. We do not need any such parameter. The deformations of the mean field in various configurations are obtained through minimization of energy, and are not additional parameters. This is somewhat like the bag model, where the radius R of the bag in each state is determined by minimizing the energy.

In Sec. II, the model is formulated and the equilibrium deformations are determined for various intrinsic states. In Sec. III, the intrinsic deformed states with proper symmetry are constructed. Some of these states are not orthogonal, since they have been generated through mean fields of different shapes. The diagonalization of the hyperfine interaction with such nonorthogonal states is described in Sec. IV. These intrinsic energies cannot be directly compared with experiment. To this end, the band-head energies are first estimated in Sec. V by calculating the moment of inertia of the deformed shape, and then forming the rotational spectrum on each band head. A very important result, already well known in nuclear physics,[4] is that the quantum-mechanical calculation for the moment of inertia of such intrinsic states is the same as the rigid moment of inertia at equilibrium deformation. Finally, in Sec. VI, a detailed comparison is made with the experimental data. It is also pointed out that a number of experimentally observed states that are difficult to explain in the conventional spherical quark model are obtained naturally through deformation.

II. THE MODEL

We consider a nonrelativistic constituent quark model in which each valence quark is moving in a deformed oscillator potential[4]

$$V(\vec{r})=\tfrac{1}{2}m(\omega_x{}^2x^2+\omega_y{}^2y^2+\omega_z{}^2z^2)\,, \tag{2.1}$$

where $\vec{r}=\vec{r}(x,y,z)$ denotes the position of the constituent quark in a body-fixed frame. The mass of the quark is denoted by m, where

$$m=m_u=m_d \tag{2.2}$$

for u- and d-type quarks (we are interested only in the strangeness-zero sector). For a set of occupied orbitals, an intrinsic state is defined, and volume conservation in the state implies that

$$\omega_x\omega_y\omega_z=\omega_0{}^3\,, \tag{2.3}$$

where ω_0 is a constant. The oscillator frequencies in the x, y, and z directions can then be parametrized as

$$\omega_x=\omega_0e^{\alpha},\quad \omega_y=\omega_0e^{\beta},\quad \omega_z=\omega_0e^{-(\alpha+\beta)}\,. \tag{2.4}$$

The single-particle eigenenergies are then given by

$$e=(n_x+\tfrac{1}{2})\hbar\omega_x+(n_y+\tfrac{1}{2})\hbar\omega_y+(n_z+\tfrac{1}{2})\hbar\omega_z\,, \tag{2.5}$$

where the n_i denote the number of excitations along the three different directions.

To begin with we assume the three quarks to be noninteracting, with each quark moving in an average deformed mean potential given by Eq. (2.1). The unperturbed part of the Hamiltonian, $\mathscr{H}_0$, is then a sum of the single-particle Hamiltonians, i.e.,

$$\mathscr{H}_0=\sum_{i=1}^{3}\left[\frac{p_i{}^2}{2m}+\frac{1}{2}m(\omega_x{}^2x_i{}^2+\omega_y{}^2y_i{}^2+\omega_z{}^2z_i{}^2)\right], \tag{2.6}$$

where $\vec{p}_i$ and $\vec{r}_i$ denote the momentum and position of the ith quark. Taking out the center-of-mass (c.m.) part we can rewrite the Hamiltonian $\mathscr{H}_0$ as

$$\mathscr{H}_0=\frac{1}{2m}(p_\rho{}^2+p_\lambda{}^2)+\tfrac{1}{2}m\sum_{i=x,y,z}\omega_i{}^2(\rho_i{}^2+\lambda_i{}^2)\,, \tag{2.7}$$

where

$$\vec{\rho}=\frac{1}{\sqrt{2}}(\vec{r}_1-\vec{r}_2),\quad \vec{\lambda}=\frac{1}{\sqrt{6}}(\vec{r}_1+\vec{r}_2-2\vec{r}_3)\,, \tag{2.8}$$

and $\vec{p}_\rho$ ($\vec{p}_\lambda$) denotes momentum conjugate to $\vec{\rho}$ ($\vec{\lambda}$). Thus we have effectively two oscillators in $\vec{\rho}$ and $\vec{\lambda}$ coordinates. The corresponding energy of the three-quark system is

$$E=\hbar\omega_0[e^{\alpha}(N_x+1)+e^{\beta}(N_y+1)+e^{-(\alpha+\beta)}(N_z+1)]\,, \tag{2.9}$$

where we have used the parametrization of Eq. (2.4) and

$$N_x=(n_{\rho_x}+n_{\lambda_x}),\quad N_y=(n_{\rho_y}+n_{\lambda_y}),\quad N_z=(n_{\rho_z}+n_{\lambda_z})\ . \tag{2.10}$$

We define $N\equiv N_x+N_y+N_z$, where N denotes the total number of excitations, and hereafter refer to α and β as the deformation parameters. Minimizing the energy E with respect to the deformation parameters α and β yields

$$\frac{\partial E}{\partial\alpha}=0,\quad \frac{\partial E}{\partial\beta}=0\ . \tag{2.11}$$

The equilibrium deformation parameters are then given by

$$\alpha=\tfrac{1}{3}\ln\left[\frac{(N_z+1)(N_y+1)}{(N_x+1)^2}\right],$$
$$\beta=\tfrac{1}{3}\ln\left[\frac{(N_z+1)(N_x+1)}{(N_y+1)^2}\right]. \tag{2.12}$$

This minimization condition may also be written as

$$\omega_x(N_x+1)=\omega_y(N_y+1)=\omega_z(N_z+1)\ . \tag{2.13}$$

Interpreted physically, the condition (2.13) implies that the density of the baryon follows the shape of the potential.[4]

In Table I we have given the equilibrium configurations and energies corresponding to $N=0,1,2$ and the lowest $N=3$ excitations of the quark orbitals. We note that as a result of the condition (2.13), the $N=0$ excitation remains spherical with

$$\omega_x=\omega_y=\omega_z=\omega_0\ . \tag{2.14}$$

The corresponding wave function will be completely symmetric, which couples to the 56 representation of the SU(6) spin-isospin group. The $N=1$ excitation turns out to be axially symmetric with one of N_x,N_y,N_z equal to unity. Thus if we choose $N_x=0$, $N_y=0$, and $N_z=1$, we have, from Eq. (2.13),

$$\omega_x=\omega_y=2\omega_z=(2)^{1/3}\omega_0\ , \tag{2.15}$$

which describes an axially symmetric prolate shape. The appropriate wave function here will have mixed-symmetry coupling to the 70 representation of SU(6).

The $N=2$ configuration once again turns out to be axially symmetric, with two possibilities: (a) $N_x=N_y=0$, $N_z=2$, which leads to a prolate shape with

$$\omega_x=\omega_y=3\omega_z=(3)^{1/3}\omega_0\ . \tag{2.16}$$

The corresponding wave function can either be fully symmetric which couples to the 56 representation of SU(6) or have mixed-symmetry coupling to the 70 representation of SU(6). (b) $N_x=N_y=1$, $N_z=0$, which leads to an oblate shape for the potential with

$$\omega_x=\omega_y=\tfrac{1}{2}\omega_z=(2)^{-1/3}\omega_0\ . \tag{2.17}$$

The wave function in this case turns out to be completely antisymmetric which couples to the 20 representation of SU(6).

The lowest $N=3$ configuration corresponds to $N_x=N_y=0$, $N_z=3$, which leads to a prolate shape with

$$\omega_x=\omega_y=4\omega_z=(4)^{1/3}\omega_0\ , \tag{2.18}$$

TABLE I. The intrinsic states in terms of the oscillator excitation quanta $N=N_x+N_y+N_z$. A given set of N_x,N_y,N_z defines an intrinsic state, the first few of which are listed in the first column. The spin-isospin multiplet structure to which it can couple is shown in the second column. The equilibrium shape is shown in the third column. The corresponding eigenenergies of $\mathscr{H}_0$ [Eq. (2.6)] at minimum are listed in the fourth column. The moment of inertia $\mathscr{I}_1$ ($=\mathscr{I}$) is evaluated from Eq. (5.4), and the factor $\hbar^2/2\mathscr{I}$ for each intrinsic state is shown in the fifth column. The last column lists $\langle L^2\rangle$, evaluated from Eq. (5.6).

Number of excitations, N	Multiplet structure (parity)	Equilibrium configuration	Intrinsic energy	$\frac{\hbar^2}{2\mathscr{I}}$	$\langle L^2\rangle$
$N=0$ $N_x=N_y=N_z=0$	$\underline{56}^+$	$\omega_x=\omega_y=\omega_z$ (spherical)	$3\hbar\omega_0$		0
$N=1$ $N_x=N_y=0,N_z=1$	$\underline{70}^-$	$\omega_x=\omega_y=2\omega_z$ (prolate)	$3.780\hbar\omega_0$	$0.126\hbar\omega_0$	3
$N=2$ $N_x=N_y=0,N_z=2$	$\underline{56}^+,\underline{70}^+$	$\omega_x=\omega_y=3\omega_z$ (prolate)	$4.327\hbar\omega_0$	$0.072\hbar\omega_0$	8
$N_x=N_y=1,N_z=0$	$\underline{20}^+$	$\omega_x=\omega_y=\frac{\omega_z}{2}$ (oblate)	$4.762\hbar\omega_0$	$0.159\hbar\omega_0$	3
$N=3$ $N_x=N_y=0,N_z=3$	$\underline{56}^-,\underline{70}^-$	$\omega_x=\omega_y=4\omega_z$ (prolate)	$4.762\hbar\omega_0$	$0.047\hbar\omega_0$	15

and the wave function could be symmetric or have mixed symmetry, with corresponding couplings to 56 or 70 representation of SU(6). We could also construct states with $N_x=0$, $N_y=1$, $N_z=2$ (triaxial), and $N_x=N_y=N_z=1$ (isotropic). But these states come very high in energy and therefore we exclude them from our analysis.

III. CONSTRUCTION OF INTRINSIC STATES

We construct the "intrinsic" wave functions of three-quark bound states starting from single-particle oscillator eigenfunctions $\psi_{n_x n_y n_z}$ listed in Table II. The intrinsic states are not eigenstates of the total L^2, but contain a superposition of states with various L values. However these intrinsic states do possess a definite permutation symmetry and are eigenstates of parity for a given N, the parity is even when N is even and odd when N is odd.

Consider first the state with $N=0$. This state comes the lowest in our scheme and is undeformed. Here only a symmetric (under permutation) configuration is possible, given by

$$\psi_{000}(\vec{r}_1)\psi_{000}(\vec{r}_2)\psi_{000}(\vec{r}_3)\ ,$$

denoted as $(\psi_{000})^3$. The normalized symmetric even-parity $N=0$ state after removing the c.m. part is given by

$$\Psi^{N=0}_{\rm sym}(\vec{\rho},\vec{\lambda})=\frac{\alpha_0^3}{\pi^{3/2}}\exp\left[-\frac{\alpha_0^2}{2}(\rho^2+\lambda^2)\right]\ , \tag{3.1}$$

where

TABLE II. Single-particle eigenfunctions of a deformed oscillator in Cartesian coordinates, with $n_x=n_y=0$ and $n_z=n$. The last column lists the appropriate Hermite polynomials $H_{n_z}(\alpha_z,z)$, which should be multiplied by the common factor $(\alpha_x\alpha_y\alpha_z/\pi^{3/2})^{1/2}\exp[-(\alpha_x^2x^2+\alpha_y^2y^2+\alpha_z^2z^2)/2]$ to get the normalized wave function $\psi_{n_x n_y n_z}$. Here α_i is given by the relation $\alpha_i^2=m\omega_i/\hbar$.

n_x	n_y	n_z	$H_{n_z}(\alpha_z,z)$
0	0	0	1
0	0	1	$\sqrt{2}\alpha_z z$
0	0	2	$\frac{1}{\sqrt{2}}(2\alpha_z^2z^2-1)$
0	0	3	$\sqrt{3}\alpha_z z\left[1-\frac{2\alpha_z^2}{3}z^2\right]$

$$\alpha_0^2=\frac{m\omega_0}{\hbar}=\frac{1}{b^2}\ . \tag{3.2}$$

The parameter b is the oscillator parameter.

Consider now the state with $N=2$ corresponding to $N_x=N_y=0$, $N_z=2$. We can construct both symmetric and mixed-symmetry configurations, taking care that the c.m. part of the wave function is in the ground state. The symmetric state is then given by the combination

$$\sqrt{2/3}(\psi_{000})^2\psi_{002}-\sqrt{1/3}\psi_{000}(\psi_{001})^2 \tag{3.3}$$

and symmetrizing it between $\vec{r}_1$, $\vec{r}_2$, and $\vec{r}_3$. Eliminating the c.m. part of the wave function, this may be written as

$$\Psi^{N=2}_{\rm sym}(\vec{\rho},\vec{\lambda})=\frac{\alpha_0^3}{\pi^{3/2}}\left[\frac{\alpha_0^2}{(3)^{2/3}}(\rho_z^2+\lambda_z^2)-1\right]\exp\left[-\frac{\alpha_0^2}{2(3)^{2/3}}[3(\rho_\perp^2+\lambda_\perp^2)+(\rho_z^2+\lambda_z^2)]\right]\ , \tag{3.4}$$

where

$$\rho_\perp^2=\rho_x^2+\rho_y^2,\quad \lambda_\perp^2=\lambda_x^2+\lambda_y^2\ . \tag{3.5}$$

Here we have used Eq. (2.16) to relate the oscillator parameters at equilibrium in the x, y, and z directions. In the same manner, the $N=2$ mixed-symmetry state is obtained by taking the combination

$$\sqrt{1/3}(\psi_{000})^2(\psi_{002})+\sqrt{2/3}\psi_{000}(\psi_{001})^2\ , \tag{3.6}$$

which automatically eliminates the c.m. part. Thus we have

$$\Psi^{N=2}_{\rho}(\vec{\rho},\vec{\lambda})=\frac{\alpha_0^3}{\pi^{3/2}}\left[\frac{2\alpha_0^2}{3^{2/3}}\rho_z\lambda_z\right]\exp\left[-\frac{\alpha_0^2}{2(3)^{2/3}}[3(\rho_\perp^2+\lambda_\perp^2)+(\rho_z^2+\lambda_z^2)]\right]\ , \tag{3.7}$$

$$\Psi^{N=2}_{\lambda}(\vec{\rho},\vec{\lambda})=\frac{\alpha_0^3}{\pi^{3/2}}\left[\frac{\alpha_0^2}{3^{2/3}}(\rho_z^2-\lambda_z^2)\right]\exp\left[-\frac{\alpha_0^2}{2(3)^{2/3}}[3(\rho_\perp^2+\lambda_\perp^2)+(\rho_z^2+\lambda_z^2)]\right]\ , \tag{3.8}$$

where the subscripts ρ,λ refer to the two possible ways of constructing the mixed-symmetry state. Note that all the wave functions given above, Eqs. (3.1)–(3.8), have $\Lambda=0$ where Λ is the projection of the total angular momentum $\vec{L}=\vec{L}_\rho+\vec{L}_\lambda$ along the body-fixed z axis.

While the $N_z=2$, $N_x=N_y=0$ states constructed above correspond to a prolate deformation ($\omega_x,\omega_y>\omega_z$), the $N_x=N_y=1$, $N_z=0$ state corresponds to an oblate deformation ($\omega_x,\omega_y<\omega_z$). The shapes of course refer to the equilibrium configuration. The oblate state can have projection $\Lambda=2,0,-2$. In the absence of a spin-orbit coupling the states corresponding to different Λ remain distinct. In our analysis we shall consider only those states[10] with $\Lambda=0$. Thus the $N=2$ oblate state turns out to be antisymmetric and is given by

$$\Psi^{N=2}_{A}(\vec{\rho},\vec{\lambda})=\frac{\alpha_0^3}{\pi^{3/2}}\frac{1}{\sqrt{2}}\frac{\alpha_0^2}{2^{1/3}}(\rho_-\lambda_+-\rho_+\lambda_-)\exp\left[-\frac{\alpha_0^2}{2(2)^{1/3}}[(\rho_\perp^2+\lambda_\perp^2)+2(\rho_z^2+\lambda_z^2)]\right]\ , \tag{3.9}$$

where we have used Eq. (2.17) and

$$\rho_{\pm}=(\rho_x \pm i\rho_y),\quad \lambda_{\pm}=(\lambda_x \pm i\lambda_y)\ . \tag{3.10}$$

We now turn to the odd-parity configurations. The $N=1$ ($N_x=N_y=0$, $N_z=1$) odd-parity state, corresponding to an axially symmetric prolate shape, can be constructed by having two quarks in the ψ_{000} state and one in the ψ_{001} state. The symmetric combination here gives just the wave function corresponding to an excitation of the c.m. and hence is not relevant. The mixed-symmetry combination yields

$$\Psi^{N=1}_{\binom{\rho}{\lambda}}(\vec{\rho},\vec{\lambda})=\frac{\alpha_0^{\,3}}{\pi^{3/2}}\sqrt{2}\frac{\alpha_0}{2^{1/3}}\begin{bmatrix}\rho_z\\ \lambda_z\end{bmatrix}\exp\left[-\frac{\alpha_0^{\,2}}{2(2)^{2/3}}[2(\rho_\perp{}^2+\lambda_\perp{}^2)+(\rho_z{}^2+\lambda_z{}^2)]\right], \tag{3.11}$$

corresponding to ρ,λ types.

The $N=3$, $N_x=N_y=0$, $N_z=3$ state can be constructed by having all the three quarks in (ψ_{001}), or one each in $\psi_{001},\psi_{002},\psi_{003}$, or two quarks in ψ_{000} and one in ψ_{003} state. The relevant superposition to eliminate the c.m. dependence in the polynomial of the symmetric state is

$$\frac{1}{\sqrt{3}}(\psi_{001})^3-\frac{1}{\sqrt{2}}\psi_{000}\psi_{001}\psi_{002}-\frac{1}{\sqrt{6}}(\psi_{000})^2\psi_{003}\ . \tag{3.12}$$

The $N=3$, prolate symmetric state with $\Lambda=0$ is then given by

$$\Psi^{N=3}_{\rm sym}(\vec{\rho},\vec{\lambda})=\frac{\alpha_0^{\,3}}{\pi^{3/2}}\frac{\alpha_0^{\,3}}{8}\left[\lambda_z{}^3+\frac{\rho_z{}^3}{3}-3\rho_z{}^2\lambda_z-\sqrt{3}\rho_z\lambda_z{}^2\right]\exp\left[-\frac{\alpha_0^{\,2}}{2(4)^{2/3}}[4(\rho_\perp{}^2+\lambda_\perp{}^2)+(\rho_z{}^2+\lambda_z{}^2)]\right]. \tag{3.13}$$

We could also construct the mixed-symmetry $N=3$ state in a similar manner. However, as the mixed-symmetry state always comes higher in energy than the symmetric state, we shall restrict our attention only to the symmetric part of the $N=3$ excitations at present and reserve our comments on the position of the $N=3$ mixed-symmetry states to the concluding remarks.

The triaxial ($N_x=0$, $N_y=1$, $N_z=2$) and the isotropic ($N_x=N_y=N_z=1$) $N=3$ states correspond to intrinsic energies $5.45\omega_0$ and $6\omega_0$. From Table I it is easily seen that these states come at least 400 and 700 MeV above the lowest $N=3$ state when $\omega_0\simeq 550$ MeV. Hence these levels can only be of academic interest at present as there are very few observed levels in this region of energies.

We are now in a position to construct the fully antisymmetric three-quark wave functions. Since the color part is always antisymmetric, it is sufficient to construct states symmetric in space, spin, and isospin coordinates. In the following we list these wave functions in which the intrinsic spatial wave function (Ψ) is coupled to the eigenfunction χ with spin $S=\frac{1}{2}$ or $\frac{3}{2}$ and to the eigenfunction ϕ with isospin $I=\frac{1}{2}$ or $\frac{3}{2}$. They are classified according to the number of excitations N, the multiplet representation of SU(6)$\otimes O(3)$, the spin S ($\frac{1}{2}$ or $\frac{3}{2}$), and isospin I ($\frac{1}{2}$ or $\frac{3}{2}$) of the state. All these states are color singlets.

(1) Even parity, $I=\frac{1}{2}$:

$$|\,56^+,N=0,S=\tfrac{1}{2},I=\tfrac{1}{2}\rangle=\frac{1}{\sqrt{2}}(\chi^\rho\phi^\rho+\chi^\lambda\phi^\lambda)\Psi^{N=0}_{\rm sym}\ , \tag{3.14}$$

$$|\,56^+,2,\tfrac{1}{2},\tfrac{1}{2}\rangle=\frac{1}{\sqrt{2}}(\chi^\rho\phi^\rho+\chi^\lambda\phi^\lambda)\Psi^{N=2}_{\rm sym}\ , \tag{3.15}$$

$$|\,70^+,2,\tfrac{1}{2},\tfrac{1}{2}\rangle=\tfrac{1}{2}[(\chi^\rho\phi^\lambda+\chi^\lambda\phi^\rho)\Psi^{N=2}_{\rho}+(\chi^\rho\phi^\rho-\chi^\lambda\phi^\lambda)\Psi^{N=2}_{\lambda}]\ , \tag{3.16}$$

$$|\,70^+,2,\tfrac{3}{2},\tfrac{1}{2}\rangle=\frac{1}{\sqrt{2}}(\phi^\rho\Psi^{N=2}_{\rho}+\phi^\lambda\Psi^{N=2}_{\lambda})\chi^s\ , \tag{3.17}$$

$$|\,20^+,2,\tfrac{1}{2},\tfrac{1}{2}\rangle=\frac{1}{\sqrt{2}}(\chi^\rho\phi^\lambda-\chi^\lambda\phi^\rho)\Psi^{N=2}_{A}\ . \tag{3.18}$$

(2) Even parity, $I=\frac{3}{2}$:

$$|\,56^+,0,\tfrac{3}{2},\tfrac{3}{2}\rangle=\Psi^{N=0}_{\rm sym}\chi^s\phi_\Delta\ , \tag{3.19}$$

$$|\,56^+,2,\tfrac{3}{2},\tfrac{3}{2}\rangle=\Psi^{N=2}_{\rm sym}\chi^s\phi_\Delta\ , \tag{3.20}$$

$$|\,70^+,2,\tfrac{1}{2},\tfrac{3}{2}\rangle=\frac{1}{\sqrt{2}}(\chi^\rho\Psi^{N=2}_{\rho}+\chi^\lambda\Psi^{N=2}_{\lambda})\phi_\Delta\ . \tag{3.21}$$

(3) Odd parity, $I=\frac{1}{2}$:

$$|\,70^-,1,\tfrac{1}{2},\tfrac{1}{2}\rangle=\tfrac{1}{2}[(\chi^\rho\phi^\lambda+\chi^\lambda\phi^\rho)\Psi^{N=1}_{\rho}+(\chi^\rho\phi^\rho-\chi^\lambda\phi^\lambda)\Psi^{N=1}_{\lambda}]\ , \tag{3.22}$$

$$|\,56^-,3,\tfrac{1}{2},\tfrac{1}{2}\rangle=\frac{1}{\sqrt{2}}(\chi^\rho\phi^\rho+\chi^\lambda\phi^\lambda)\Psi^{N=3}_{\rm sym}\ , \tag{3.23}$$

$$|\,70^-,1,\tfrac{3}{2},\tfrac{1}{2}\rangle=\frac{1}{\sqrt{2}}(\phi^\rho\Psi^{N=1}_{\rho}+\phi^\lambda\Psi^{N=1}_{\lambda})\chi^s\ . \tag{3.24}$$

(4) Odd parity, $I=\frac{3}{2}$:

$$|\,70^-,1,\tfrac{1}{2},\tfrac{3}{2}\rangle=\frac{1}{\sqrt{2}}(\chi^\rho\Psi^{N=1}_{\rho}+\chi^\lambda\Psi^{N=1}_{\lambda})\phi_\Delta\ , \tag{3.25}$$

$$|\,56^-,3,\tfrac{3}{2},\tfrac{3}{2}\rangle=\Psi^{N=3}_{\rm sym}\chi^s\phi_\Delta\ . \tag{3.26}$$

The spin (χ) and isospin (ϕ) wave functions for the states with maximum projection are given by

$$\begin{aligned}\chi^\rho_{+1/2}&=\frac{1}{\sqrt{2}}(\uparrow\downarrow\uparrow-\downarrow\uparrow\uparrow)\ ,\\ \chi^\lambda_{+1/2}&=\frac{1}{\sqrt{6}}(\uparrow\downarrow\uparrow+\downarrow\uparrow\uparrow-2\uparrow\uparrow\downarrow)\ ,\\ \chi^s_{+3/2}&=\uparrow\uparrow\uparrow\ ,\end{aligned} \tag{3.27}$$

where $\uparrow(\downarrow)$ denotes the single-particle spin state with projection $+\frac{1}{2}(-\frac{1}{2})$ and

$$\phi_p^\rho=\frac{1}{\sqrt{2}}(udu-duu),\quad \phi_p^\lambda=\frac{-1}{\sqrt{6}}(udu+duu-2uud)\ ,$$
$$\phi_\Delta=uuu\ , \tag{3.28}$$

where u and d denote the up and down quarks. The states with less than maximum projection are obtained by using step-down operators in spin and isospin.

IV. DIAGONALIZATION

We follow a two-step procedure to obtain the spectra of $N\leq 3$ baryons. First, we diagonalize the full Hamiltonian in the space of intrinsic states and obtain the intrinsic energies as well as mixing among the various intrinsic states. Second, we assume that the states when projected onto states of good L yield the characteristic rotational spectra built on the appropriate band head. This assumption is valid when the states are sufficiently deformed, as in our case, and when the collective rotational motion of the state as a whole does not perturb the internal motion. The different total angular momentum states are then obtained by coupling a particular $\vec{L}$ to a given total spin $\vec{S}$. These states are, however, degenerate when they are obtained from the same $\vec{L}$ and $\vec{S}$.

The form of the Hamiltonian is chosen to be

$$\mathscr{H}=3m+\mathscr{H}_0+\mathscr{H}_c+\sum_{i<j}^{3}U(\vec{r}_{ij})+\Delta\ , \tag{4.1}$$

where $\mathscr{H}_0$, given by Eq. (2.7), is the unperturbed part of the Hamiltonian whose eigenstates now form the basis for diagonalizing $\mathscr{H}$. The spin-spin contact force $\mathscr{H}_c$ is given by

$$\mathscr{H}_c=\sum_{i<j}^{3}\frac{16\alpha_s\pi}{9m^2}\vec{S}_i\cdot\vec{S}_j\delta^3(\vec{r}_{ij})\ , \tag{4.2}$$

where

$$\vec{r}_i=\vec{r}_i-\vec{r}_j\ , \tag{4.3}$$

$$\vec{S}_i=\tfrac{1}{2}\vec{\sigma}_i\ , \tag{4.4}$$

and α_s is the strong coupling constant. Utilizing the symmetry of the wave function under the exchange of space, spin, and isospin coordinates we can rewrite[8] $\mathscr{H}_c$ as

$$\mathscr{H}_c=\frac{4\sqrt{2}\alpha_s\pi}{3m^2}\vec{S}_1\cdot\vec{S}_2\delta^3(\vec{\rho})\ . \tag{4.5}$$

The matrix elements of $\mathscr{H}_c$ among intrinsic states are given in Table III. The $U(\vec{r}_{ij})$ in Eq. (4.1) effectively takes care of any short-range two-body interaction that might have been excluded from the mean field. The necessity to introduce $U(\vec{r}_{ij})$ arises for the following reason. If we start with the intrinsic Hamiltonian $\mathscr{H}_0$, the $N=2$ symmetric and mixed-symmetry states are degenerate. The degeneracy is split by the spin-spin force. However, any spin-spin interaction, whose strength is adjusted to obtain $N(940)$ and $\Delta(1232)$ mass difference, cannot at the same time reproduce the difference in masses between the $N(1440)$, which is mostly symmetric, and the $N(1710)$ which is mainly a mixed-symmetry state. Such a splitting can only be achieved by a weak, attractive, possibly short-range central interaction. Without any loss of generality we can choose $U(\vec{r}_{ij})$ to be

$$\sum_{i<j}^{3}U(\vec{r}_{ij})=3U(\sqrt{2}\vec{\rho})=-A\delta(\vec{\rho})\ , \tag{4.6}$$

where A denotes the strength. We could have chosen a more general form for $U(\vec{r}_{ij})$, which will effectively involve matrix elements of an operator[11] $\sum_n\beta_n(\vec{\rho}\cdot\vec{\rho})^n$. However, some of these matrix elements can be taken care of by redefining the oscillator parameter ω_0 as an effective Ω.[8,9,12] As far as first-order perturbation involving only the diagonal matrix elements is concerned this generalization leads to essentially the same results as in the case of an attractive δ-function force. This equality breaks down when the mixing among various intrinsic levels due to the off-diagonal matrix elements is considered. We stick to the first-order perturbation with the form given by Eq. (4.6). This is partially justified in our model since (a) we have chosen a comparatively weak $U(\vec{r}_{ij})$, and (b) the off-diagonal matrix element is zero in most cases due to spin-isospin orthogonality except between the states with same permutation symmetry, spin, and isospin like the $N=0$, $\underline{56}^+$ and $N=2$, $\underline{56}^+$ states. Also the effect of off-diagonal matrix elements cannot be completely estimated unless we have a larger space of basis states.

We thus obtain

$$\sum_{i<j}\langle N=0,56^+\,|\,U(\vec{r}_{ij})\,|\,N=0,56^+\rangle=\delta\ , \tag{4.7}$$

$$\sum_{i<j}\langle N=1,70^-\,|\,U(\vec{r}_{ij})\,|\,N=1,70^-\rangle=\frac{\delta}{2}\ , \tag{4.8}$$

$$\sum_{i<j}\langle N=2,56^+\,|\,U(\vec{r}_{ij})\,|\,N=2,56^+\rangle=\tfrac{3}{4}\delta\ , \tag{4.9}$$

$$\sum_{i<j}\langle N=2,70^+\,|\,U(\vec{r}_{ij})\,|\,N=2,70^+\rangle=\tfrac{3}{8}\delta\ , \tag{4.10}$$

$$\sum_{i<j}\langle N=2,20^+\,|\,U(\vec{r}_{ij})\,|\,N=2,20^+\rangle=0\ , \tag{4.11}$$

$$\sum_{i<j}\langle N=3,56^-\,|\,U(\vec{r}_{ij})\,|\,N=3,56^-\rangle=\tfrac{15}{32}\delta\ . \tag{4.12}$$

Hereafter, we shall treat δ as a parameter which eliminates the need to determine the strength A of $U(\vec{r}_{ij})$. The overall constant Δ in Eq. (4.1) is fixed at -1276 MeV to give the mass of the nucleon ground state to be 940 MeV. The spin-orbit interaction is neglected for reasons explained in I. The tensor coupling is also ignored as there is evidence to believe that it is small.[9] As a result of this assumption, there is no mixing between states of $S=\frac{1}{2}$ and $S=\frac{3}{2}$. If this assumption is not made, then one can construct a strong-coupling model for the deformed states, as was done in Ref. 13.

The set of intrinsic states given by Eqs. (3.14)—(3.26) provide the basis for diagonalizing $\mathscr{H}$. Not all these states are however mutually orthogonal; the $N=0$ symmetry state is not orthogonal to its nodal excitation $N=2$ symmetric state, when the spin and isospin are the same.

TABLE III. Matrix elements of the spin-spin contact potential $\mathscr{H}_c$ [Eq. (4.5)] between relevant intrinsic states [given in Eqs. (3.14)—(3.26)] in units of $\sqrt{2}\alpha_s/3m^2\sqrt{\pi}$. Here we have used the parameters β_N and γ_N, defined by the relations $\beta_N{}^2=(N+1)\gamma_N{}^2=(N+1)^{1/3}\alpha_0{}^2$, with $\alpha_0{}^2=m\omega_0/\hbar$. The four matrices displayed are for the even-parity nucleon and Δ, and the odd-parity nucleon and Δ states, respectively.

1. $|56,0,\frac{1}{2},\frac{1}{2}\rangle$ $|56^+,2,\frac{1}{2},\frac{1}{2}\rangle$ $|70^+,2,\frac{1}{2},\frac{1}{2}\rangle$ $|70^+,2,\frac{3}{2},\frac{1}{2}\rangle$

$$\begin{bmatrix} -\beta_0{}^2\gamma_0 & \frac{2\sqrt{2}\beta_2{}^2\beta_0{}^2\gamma_2\gamma_0{}^3}{(\beta_2{}^2+\beta_0{}^2)(\gamma_2{}^2+\gamma_0{}^2)^{3/2}} & \frac{4\beta_2{}^2\beta_0{}^2\gamma_2{}^3\gamma_0}{(\beta_2{}^2+\beta_0{}^2)(\gamma_2{}^2+\gamma_0{}^2)^{3/2}} & 0 \\ \frac{2\sqrt{2}\beta_2{}^2\beta_0{}^2\gamma_2\gamma_0{}^3}{(\beta_2{}^2+\beta_0{}^2)(\gamma_2{}^2+\gamma_0{}^2)^{3/2}} & -\frac{3}{4}\beta_2{}^2\gamma_2 & \frac{1}{2\sqrt{2}}\beta_2{}^2\gamma_2 & 0 \\ +\frac{4\beta_2{}^2\beta_0{}^2\gamma_2{}^3\gamma_0}{(\beta_2{}^2+\beta_2{}^2)(\gamma_2{}^2+\gamma_0{}^2)^{3/2}} & \frac{1}{\sqrt{2}}\beta_2{}^2\gamma_2 & -\frac{3}{8}\beta_2{}^2\gamma_2 & 0 \\ 0 & 0 & 0 & \frac{3}{8}\beta_2{}^2\gamma_2 \end{bmatrix} \begin{matrix} |56^+,0,\frac{1}{2},\frac{1}{2}\rangle \\ |56^+,2,\frac{1}{2},\frac{1}{2}\rangle \\ |70^+,2,\frac{1}{2},\frac{1}{2}\rangle \\ |70^+,2,\frac{3}{2},\frac{1}{2}\rangle \end{matrix}$$

2. $|56^+,0,\frac{3}{2},\frac{3}{2}\rangle$ $|56^+,2,\frac{3}{2},\frac{3}{2}\rangle$ $|70^+,2,\frac{1}{2},\frac{3}{2}\rangle$

$$\begin{bmatrix} +\beta_0{}^2\gamma_0 & -\frac{2\sqrt{2}\beta_2{}^2\beta_0{}^2\gamma_2\gamma_0{}^3}{(\beta_2{}^2+\beta_0{}^2)(\gamma_2{}^2+\gamma_0{}^2)^{3/2}} & 0 \\ -\frac{2\sqrt{2}\beta_2{}^2\beta_0{}^2\gamma_2\gamma_0{}^3}{(\beta_2{}^2+\beta_0{}^2)(\gamma_2{}^2+\gamma_0{}^2)^{3/2}} & \frac{3}{4}\beta_2{}^2\gamma_2 & 0 \\ 0 & 0 & \frac{3}{8}\beta_2{}^2\gamma_2 \end{bmatrix} \begin{matrix} |56^+,0,\frac{3}{2},\frac{3}{2}\rangle \\ |56^+,2,\frac{3}{2},\frac{3}{2}\rangle \\ |70^+,2,\frac{1}{2},\frac{3}{2}\rangle \end{matrix}$$

3. $|70^-,1,\frac{1}{2},\frac{1}{2}\rangle$ $|70^-,1,\frac{3}{2},\frac{1}{2}\rangle$ $|56^-,3,\frac{1}{2},\frac{1}{2}\rangle$

$$\begin{bmatrix} -\frac{\beta_1{}^2\gamma_1}{2} & 0 & -\frac{6\sqrt{2}\beta_1{}^2\beta_3{}^2\gamma_1{}^2\gamma_3{}^4}{(\beta_1{}^2+\beta_3{}^2)(\gamma_1{}^2+\gamma_3{}^2)^{5/2}} \\ 0 & \frac{\beta_1{}^2\gamma_1}{2} & 0 \\ -\frac{6\sqrt{2}\beta_1{}^2\beta_3{}^2\gamma_1{}^2\gamma_3{}^4}{(\beta_1{}^2+\beta_3{}^2)(\gamma_1{}^2+\gamma_3{}^2)^{5/2}} & 0 & -\frac{15}{32}\beta_3{}^2\gamma_3 \end{bmatrix} \begin{matrix} |70^-,1,\frac{1}{2},\frac{1}{2}\rangle \\ |70^-,1,\frac{3}{2},\frac{1}{2}\rangle \\ |56^-,3,\frac{1}{2},\frac{1}{2}\rangle \end{matrix}$$

4. $|70^-,1,\frac{1}{2},\frac{3}{2}\rangle$ $|56^-,3,\frac{3}{2},\frac{3}{2}\rangle$

$$\begin{bmatrix} \frac{\beta_1{}^2\gamma_1{}^2}{2} & 0 \\ 0 & +\frac{15}{32}\beta_3{}^2\gamma_3 \end{bmatrix} \begin{matrix} |70^-,1,\frac{1}{2},\frac{3}{2}\rangle \\ |56^-,3,\frac{3}{2},\frac{3}{2}\rangle \end{matrix}$$

This is due to the fact that the $N=0$ and the $N=2$ states have been generated through mean fields of different shape. To overcome this problem we rewrite the unperturbed part of the Hamiltonan $\mathscr{H}_0$ as

$$\mathscr{H}_0=\tfrac{1}{2}(\overrightarrow{\mathscr{H}}_0+\overleftarrow{\mathscr{H}}_0)\ , \tag{4.13}$$

where the direction of the arrow indicates whether $\mathscr{H}_0$ operates to the right or to the left. The diagonal matrix elements of $\mathscr{H}_0$ are unchanged by this prescription and the corresponding energies are given in Table I. Note that these energies have been obtained after eliminating the c.m. contribution. $\mathscr{H}_0$ has a nonzero off-diagonal matrix element only between the $N=0$ symmetric state and its nodal excitation $N=2$ symmetric state, given by

$$\langle 56,0,S,I\,|\,\mathscr{H}_0\,|\,56,2,S,I\rangle = \tfrac{1}{2}(E_0+E_2)\langle 56,0,S,I\,|\,56,2,S,I\rangle\ , \tag{4.14}$$

where

$$\langle 56,0,S,I\,|\,56,2,S,I\rangle=-0.3172\ . \tag{4.15}$$

The eigenvalues and eigenvectors of $\mathscr{H}$ are found by using the standard method[14] of diagonalization from a nonorthogonal basis. The eigenvalues are found by solving the determinantal equation

$$\det(\mathscr{H}_{ij}-EN_{ij})=0\ , \tag{4.16}$$

where $\mathscr{H}_{ij}$ denotes the (i,j)th matrix element of $\mathscr{H}$ and (N_{ij}) is the overlap matrix. If we had neglected the

TABLE IV. The normalized intrinsic wave functions and the corresponding energies after diagonalization of $\mathscr{H}$ [Eqs. (4.1) and (4.16)]. Note that the amplitude of a state may exceed unity in a nonorthogonal basis.

Intrinsic energy (MeV)	Wave function					
940	1.038	0.174	−0.089	0	0	$\|56^+,0,\frac{1}{2},\frac{1}{2}\rangle$
1786	0.111	0.939	−0.415	0	0	$\|56^+,2,\frac{1}{2},\frac{1}{2}\rangle$
1989	0.153	0.447	0.906	0	0	$\|70^+,2,\frac{1}{2},\frac{1}{2}\rangle$
2076	0	0	0	1	0	$\|70^+,2,\frac{3}{2},\frac{1}{2}\rangle$
2333	0	0	0	0	1	$\|20^+,2,\frac{1}{2},\frac{1}{2}\rangle$
1230	1.055	0.344	0			$\|56^+,0,\frac{3}{2},\frac{3}{2}\rangle$
2059	−0.009	0.997	0			$\|56^+,2,\frac{3}{2},\frac{3}{2}\rangle$
2076	0	0	1			$\|70^+,2,\frac{1}{2},\frac{3}{2}\rangle$
1579	0.986	0	0.167			$\|70^-,1,\frac{1}{2},\frac{1}{2}\rangle$
1769	0	1	0			$\|70^-,1,\frac{3}{2},\frac{1}{2}\rangle$
2164	−0.167	0	0.986			$\|56^-,3,\frac{1}{2},\frac{1}{2}\rangle$
1769	1	0	$\|70^-,1,\frac{1}{2},\frac{3}{2}\rangle$			
2164	0	1	$\|56^-,3,\frac{3}{2},\frac{3}{2}\rangle$			

nonzero overlap between 56 $N=0$ and $N=2$ states, (N_{ij}) would reduce to the unit matrix (δ_{ij}), and Eq. (4.16) then is the simple eigenvalue equation.

The results of the diagonalization are given in Table IV. The energies quoted correspond to the intrinsic energies of the states with respect to which $\mathscr{H}$ assumes a diagonal form. For the $N=0$ state, however, the intrinsic energy itself corresponds to the physical mass since it is spherical in our model. The parameters of the fit are the constituent quark mass m, the oscillator parameter b (or $1/\alpha_0$), the strong coupling constant α_s, the overall constant Δ. The quark mass is chosen to be 330 MeV as suggested by magnetic-moment calculations for proton and neutron in the nonrelativistic constituent quark model. The oscillator parameter b and the strong coupling constant α_s are fixed at 0.4631 fm and 0.92, respectively, to yield the nucleon ($N=0$) and Δ ($N=0$) mass difference to be approximately 300 MeV. The corresponding $\hbar\omega_0$ is about 550 MeV, which yields the $N=1$ odd-parity states at about the right energy. The overall constant Δ is fixed so as to get the nucleon ($N=0$) mass at 940 MeV. It turns out that $\Delta=-1276$ MeV.

Note that because our $U(\vec{r}_{ij})$ is rather weak, we find a substantial mixing between the 56 $N=2$ and 70 $N=2$ states. This mixing seems to be essential if we have to explain the radiative decay strengths for $N(1440)\to N(940)+\gamma$ and $N(1710)\to N(940)+\gamma$ as discussed in Ref. 1.

V. ROTATIONAL SPECTRA

The intrinsic wave functions outlined in Sec. III contain a superposition of states of orbital angular momentum $L=0,2,4,\ldots$ in the even-parity prolate states and $L=1,3,5,\ldots$ in the odd-parity prolate or even-parity oblate states. With intrinsic states sufficiently deformed, projection onto states of good L generates[7] the characteristic rotational spectrum built on a particular band head. The energy of the band head (i.e., the state with the lowest L) is obtained using the rotor model as

$$E(L=0)=E_{\text{intrinsic}}-\frac{\hbar^2\langle L^2\rangle}{2\mathscr{I}} \tag{5.1}$$

for the even-parity prolate bands, and

$$E(L=1)=E_{\text{intrinsic}}+\frac{\hbar^2}{2\mathscr{I}}\{2-\langle L^2\rangle\} \tag{5.2}$$

for odd-parity prolate bands and the $N=2$ oblate band. The states of higher L are obtained by noting that the energy increases as

$$\frac{\hbar^2}{2\mathscr{I}}L(L+1)$$

in each band. Note that the effect of removing $\hbar^2\langle L^2\rangle/2\mathscr{I}$ is to eliminate any contribution coming from the intrinsic state to the rotational energy. The moment of inertia (about an axis perpendicular to the symmetry axis) of the particular band is denoted by $\mathscr{I}_1$, and a quantum-mechanical expression for $\mathscr{I}_1$ can be obtained starting from the independent-particle approximation, given by[4]

$$\mathscr{I}_1=\frac{\hbar}{2\omega_y\omega_z}\left[\frac{(\omega_y+\omega_z)^2}{(\omega_y-\omega_z)}(N_z-N_y)+\frac{(\omega_y-\omega_z)^2}{(\omega_y+\omega_z)}(N_y+N_z+2)\right], \tag{5.3}$$

where the moment of inertia is defined with respect to the x axis. At equilibrium the expression (5.3) for the moment of inertia reduces to

$$\frac{\mathcal{I}_1}{\hbar}=\frac{(N_z+1)}{\omega_z}+\frac{(N_y+1)}{\omega_y}\ . \tag{5.4}$$

By symmetry we can easily write down the expression for moment of inertia about other axes. However, all the cases we are interested in possess an axial symmetry (except $N=0$ which is isotropic), in which we have chosen the z axis to be the axis of symmetry. In such cases, $\mathcal{I}=\mathcal{I}_1=\mathcal{I}_2$, and $\mathcal{I}_3$ will be undefined. This is easily understood since any rotation around the symmetry axis leaves the system invariant. Thus the rotational spectra correspond to collective rotations about an axis perpendicular to the axis of symmetry. We also observe that at equilibrium the moment of inertia given by Eq. (5.4) is identically equal to the rigid moment of inertia. The moment of inertia in terms of ω_0 is explicitly given in Table I.

The expectation value $\langle L^2\rangle$, where

$$\vec{\mathrm{L}}=\vec{\mathrm{L}}_\rho+\vec{\mathrm{L}}_\lambda\ , \tag{5.5}$$

turns out to be independent of the oscillator parameter and is purely a function of the deformation. For an axially symmetric solution at equilibrium deformation, the expectation value of $\langle L^2\rangle$ is given by the simple expression

$$\langle L^2\rangle=(\omega_>/\omega_<)^2-1\ , \tag{5.6}$$

where $\omega_>$ ($\omega_<$) is the larger (smaller) of $\omega_\perp$ ($=\omega_x=\omega_y$) and ω_z. The ratio ($\omega_>/\omega_<$) is an integer at equilibrium, and the corresponding value of $\langle L^2\rangle$ for various intrinsic states are listed in Table I.

VI. COMPARISON WITH EXPERIMENTAL RESULTS

The results of our fits to baryon masses are given in Figs. 1–4. We have employed the spectroscopic notation[15] to identify levels. The full circles in the figures correspond to the nominal masses of the states used for identification while the range is denoted by vertical bars. Wherever the bars are not shown it should be assumed that it is a weak (one or two star) state. The theoretical predictions are shown by horizontal lines.

Figure 1 shows the even-parity $I=\frac{1}{2}$ spectra. The experimental levels are grouped according to the proposed rotational bands.[1] The $N=0$ nucleon state is fixed at 940 MeV by the choice of the overall constant Δ, and is not shown in the figure. The $N=2$ excitation spectrum is divided into four bands, a symmetric $\underline{56}$ band coupled to $S=\frac{1}{2}$ [Fig. 1(a)], a mixed-symmetry $\underline{70}$ band coupled to $S=\frac{1}{2}$ [Fig. 1(b)], and $S=\frac{3}{2}$ [Fig. 1(c)], and an antisymmetric $\underline{20}$ band coupled to total spin $S=\frac{1}{2}$ whose band head is shown by a dashed line in Fig. 1(c). The agreement in the symmetric $\underline{56}$ band between the theoretical and experimental levels is fairly good, though the $L=4$, F_{17} state is yet to be found. In the mixed-symmetry $S=\frac{1}{2}$ and $\frac{3}{2}$ bands only two states $P_{11}(1710)$ and $F_{17}(1990)$ have been established with certainty, and their observed masses are in reasonable agreement with our model. The weak F_{15} state at 2000 MeV can be included in either of these two mixed-symmetry bands. Similarly the weak P_{11} state at 2100 MeV can be included either in the mixed-symmetry $\underline{70}$, $S=\frac{3}{2}$ band or in the antisymmetric $\underline{20}$, $S=\frac{1}{2}$ band. Such ambiguities as these cannot be resolved at present. Note that the $\underline{20}^+$ states do not mix with either the $\underline{70}^+$ or with the $\underline{56}^+$ states through spin-spin interaction. In fact, even the diagonal matrix elements of H_c and $U(\vec{r}_{ij})$ are zero for a $\underline{20}^+$ state. This is precisely the reason why the band head with $L=1$ for the $\underline{20}^+$ comes at about 2250 MeV. Since the parameter $\hbar^2/2\mathcal{I}_1$ for this band is about 87 MeV, the next member of the band with $L=3$ is pushed up by 870 MeV.

The relatively fewer number of states seen in the even-parity mixed-symmetry configuration is due to the fact

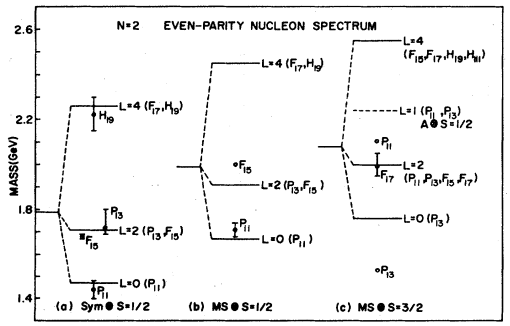

FIG. 1. Even-parity $N=2$ nucleon spectra (a) symmetric, $S=\frac{1}{2}$ band, (b) mixed symmetry, $S=\frac{1}{2}$ band, (c) mixed symmetry, $S=\frac{3}{2}$ band. The lowest $L=1$ band head of the $\underline{20}^+$ antisymmetric band is shown by the dashed line in (c). The nominal masses (Ref. 15) of well-defined states are shown by full circles, while the masses of the weak states are shown by open circles. The position of the intrinsic state is also shown for each band.

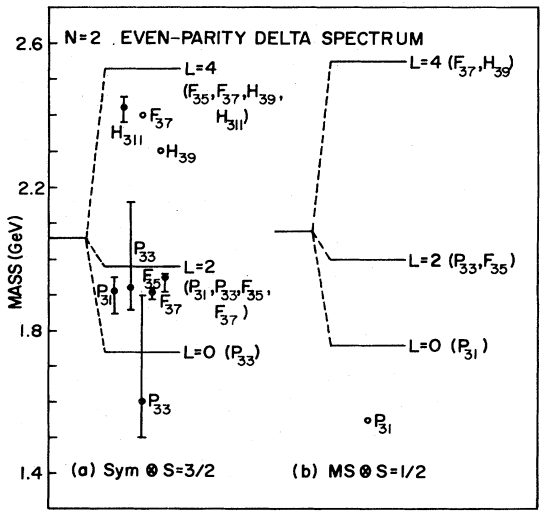

FIG. 2. Even-parity $N=2$ Δ spectra, (a) symmetric, $S=\frac{3}{2}$ band, (b) mixed symmetry, $S=\frac{1}{2}$ band. The notation is the same as in Fig. 1.

that these couple weakly to the π-N elastic channel compared to the symmetric states. A slight enhancement however occurs due to configuration mixing with the states of the symmetric band (see Table IV).

The even-parity Δ states are shown in Fig. 2. There are only two bands here: (a) the symmetric $\underline{56}$, $S=\frac{3}{2}$ band shown in Fig. 2(a), and (b) the mixed-symmetry $\underline{70}$, $S=\frac{1}{2}$ band shown in Fig. 2(b). As in the $I=\frac{1}{2}$ symmetric band, there is good agreement between the experimental states and the theoretical calculations in the $I=\frac{3}{2}$ symmetric band. Corresponding to the mixed symmetry, $S=\frac{1}{2}$ band there are no observed levels to compare except a weak P_{31} at 1550 MeV.

We shall now turn our attention to the odd-parity states. The $I=\frac{1}{2}$ spectrum is shown in Fig. 3. The mixed-symmetry $\underline{70}$, $S=\frac{1}{2}$ band is shown in Fig. 3(a). The band head corresponding to $L=1$, S_{11} and D_{13} states comes at 1510 MeV, close to the observed levels. The interesting thing to notice in this band is however the $L=3$, D_{15} and G_{17} levels at 2200 MeV, almost exactly corresponding to the observed masses. Unlike the spherical oscillator model,[9] where these belong to the $N=3$ mixed-symmetry levels, these states are explained in our model as belonging to the $N=1$ mixed-symmetry rotational band. The fact that these states are strongly seen perhaps justifies this inclusion in the $N=1$ band rather than the $N=3$ band.

In Fig. 3(b) we have shown the mixed-symmetry $\underline{70}$, $N=1$, $S=\frac{3}{2}$ band. The agreement with $L=1$ levels is good while the $L=3$ states have not been seen except for a G_{19} state at 2250 MeV. In Fig. 3(c), the symmetric $\underline{56}$, $N=3$, $S=\frac{1}{2}$ band is shown. There is a weak D_{13} state at 1880 MeV (shown by an open square) according to the analysis of Ref. 16, which corresponds to the band head at 1830 MeV. In general the states in this band couple rather weakly to the π-N elastic and inelastic channels compared to the $\underline{70}$ $N=1$ states.[9]

Even though we have not included the mixed symmetry $\underline{70}$, $N=3$ band in our analysis, a few comments are in order. The $L=1$ band head of this band comes at 2010 MeV with our parameters if we ignore the effects of spin-spin and $U(\vec{r}_{ij})$ parts of the Hamiltonian. However, these constitute a smaller (about half) effect on a mixed-symmetry configuration than on a symmetric configuration. Thus the $I=\frac{1}{2}$, mixed-symmetry $\underline{70}$, $N=3$, $L=1$ state would be approximately found at about 2000 MeV, corresponding to $J=\frac{1}{2}$, (S_{11}) and $\frac{3}{2}$ (D_{13}). There are two observed levels corresponding to this at 2060 ± 80 MeV (D_{13}) and a weak level at 2100 MeV (S_{11}). The $L=5$ level would fit the I_{111} level shown at 2600 MeV in Fig. 3(c) and the G_{19} level at 2800 MeV. This is not an unambiguous identification since these two observed states could as well belong to the $L=5$ symmetric, $N=3$ band. The former identification is preferable, since in the odd-parity configurations, the mixed-symmetry states are seen more strongly.

The odd-parity $I=\frac{3}{2}$ spectrum is displayed in Fig. 4. Figure 4(a) shows the mixed-symmetry, $N=1$, $S=\frac{1}{2}$ band and Fig. 4(b) shows the symmetric, $N=3$, $S=\frac{3}{2}$ band. Though the higher L ($L\geq3$) states are not seen very well, the agreement is satisfactory. It is gratifying to note that the $L=1$ states of the $N=3$ band have come down in energy due to deformation.

As in the $I=\frac{1}{2}$ odd-parity $N=3$ case, we could construct an $I=\frac{3}{2}$, $N=3$, mixed-symmetry $\underline{70}$, $S=\frac{1}{2}$ band. The band head here would be at about 2100 MeV, corresponding to $J=\frac{1}{2}$ (S_{31}) and $J=\frac{3}{2}$ (D_{33} states). A weak S_{31} state is seen at 2150 MeV. The next $L=3$ and $L=5$ states would come at about 2350 and 2800 MeV. Thus the I_{313} level at 2750 MeV, shown in Fig. 4(b), may as well belong to this band.

In the spherical-oscillator model[8,9] the $N=2$ and $N=3$ states come too high in excitation energy. These are brought down by introducing a strong spin-independent central interaction $U(\vec{r}_{ij})$ which is treated only in first-order perturbation theory. This is supposed to simulate the anharmonic terms in the interquark interaction, and the energy shift due to this to the $N=2$ symmetric state is of the order of $\hbar\omega$.[17] As mentioned earlier, this prescrip-

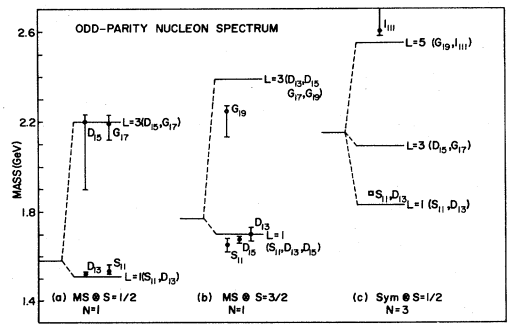

FIG. 3. Odd-parity nucleon spectra, (a) $N=1$ mixed symmetry, $S=\frac{1}{2}$ band, (b) $N=1$ mixed symmetry, $S=\frac{3}{2}$ band, (c) $N=3$, symmetric $S=\frac{1}{2}$ band. The state denoted by an open square in (c) corresponds to the phase-shift analysis of Ref. 16. The rest of the notation is the same as in earlier figures.

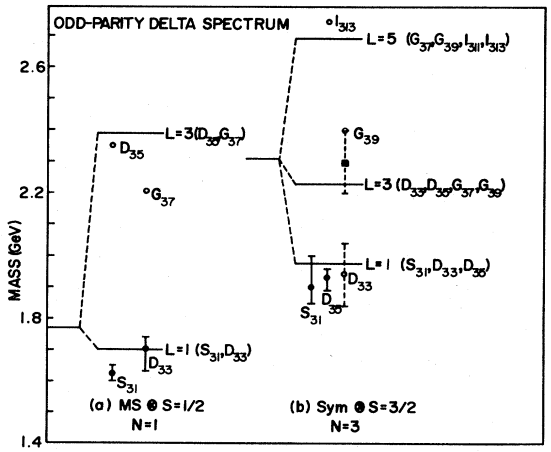

FIG. 4. Odd-parity Δ spectra, (b) $N=1$, mixed symmetry, $S=\frac{1}{2}$ band, (b) $N=3$, symmetric, $S=\frac{3}{2}$ band. The dashed vertical lines show the mass spread of the particular states according to the phase-shift analysis of Ref. 16.

tion does not fully explain the lowering of the $N=3$ odd-parity states in the Δ.[9] In our model, the lowering of the excited states is caused by the deformation of the mean field. This deformation may partly be due to the anharmonic components of the force. The residual interaction $U(\vec{r}_{ij})$ in our model is only half as strong, and a perturbation treatment with it is less objectionable. It also plays a limited role in our model, and was not included in the original version.[1] Without $U(\vec{r}_{ij})$, the splitting between the $N=2$ symmetric and mixed-symmetry $\frac{1}{2}^+$ states would only be about 160 MeV.

It is our view that deformation of the baryon even in low-lying excited states is a real physical effect, and we have demonstrated this phenomenologically by grouping the observed states in rotational bands. Once the self-consistency between the shape of density and the mean field is demanded, the quantum-mechanical moment of inertia becomes the same as the rigid-body inertia. This is just of the right magnitude needed to explain the spacing between the observed states. In the present model, the effect of interquark forces is put in indirectly through the volume conservation condition, which makes the baryonic matter incompressible. It would be desirable to perform a microscopic self-consistent calculation with a reasonable Hamiltonian to derive the mean field and demonstrate that it is deformed in excited configurations. Our more phenomenological approach may well provide the motivation for this.

ACKNOWLEDGMENTS

We are grateful to Byron Jennings for many valuable suggestions. Two of us (M.D. and J.D.) thank C. Forsyth and J. LeTourneux for useful discussions. R.K.B. and M.V.N. are grateful to Nathan Isgur and Yuki Nogami for some clarifications. This research was supported by a grant from the Natural Sciences and Engineering Research Council of Canada.

---

*Present address: Nuclear Physics Laboratory, University of Montreal, Montreal, P.Q., Canada H3C 3J7.

[1]R. K. Bhaduri, B. K. Jennings, and J. C. Waddington, Phys. Rev. D **29**, 2051 (1984).

[2]T. A. DeGrand and R. L. Jaffe, Ann. Phys. (N.Y.) **100**, 425 (1976).

[3]K. Hahn, R. Goldflam, and L. Wilets, Phys. Rev. D **27**, 269 (1983). R. D. Viollier, S. A. Chin, and A. K. Kerman, Nucl. Phys. **A407**, 269 (1983); R. Shanker, D. Vasak, C. S. Warke, W. Greiner, and B. Müller, Z. Phys. C **18**, 327 (1983).

[4]A. Bohr and B. R. Mottelson, *Nuclear Structure* (Benjamin, Reading, Mass., 1975), Vol. II, p. 77; B. R. Mottelson and S. G. Nilsson, K. Dan. Vidensk. Selsk. Mat. Fys. Skr. **1**, No. 8 (1959).

[5]J. Treiner, H. Krivine, and O. Bohigas, Nucl. Phys. **A371**, 253 (1981).

[6]R. K. Bhaduri, J. Dey, and M. A. Preston, Phys. Lett. **136B**, 289 (1984).

[7]R. E. Peierls and J. Yoccoz, Proc. Phys. Soc. London **70**, 381 (1957). See also M. A. Preston and R. K. Bhaduri, *Structure of the Nucleus* (Addison-Wesley, Reading, Mass., 1975), Chaps. 9 and 10.

[8]N. Isgur and G. Karl, Phys. Rev. D **18**, 4187 (1978); **19**, 2653 (1979); N. Isgur, in *The New Aspects of Subnuclear Physics,* proceedings of the Sixteenth International School of Subnuclear Physics, Erice, 1978, edited by A. Zichichi (Plenum, New York, 1980), p. 107.

[9]C. P. Forsyth and R. E. Cutkosky, Z. Phys. C **18**, 219 (1983).

[10]On projection, an antisymmetric intrinsic state with $\Lambda=\pm 2$ gives rise to rotational bands with $L=3$ as the lowest angular momentum state. This comes several hundred MeV higher than the $L=1$ state in the $\Lambda=0$ band considered in the text.

[11]K. C. Bowler and B. F. Tynemouth, Phys. Rev. D **27**, 662 (1983).

[12]K. C. Bowler, P. J. Corvi, A. J. G. Hey, and P. D. Jarvis, Phys. Rev. D **24**, 197 (1981).

[13]R. K. Bhaduri, B. K. Jennings, and J. C. Waddington, TRIUMF Report No. TRI-pp-83-50 (unpublished); in *MRST 83,* proceedings of the Fifth Annual Montreal-Syracuse-Rochester-Toronto Meeting, Toronto, 1983, edited by G. Kunstatter and P. J. O'Donnell (University of Toronto Press, Toronto, 1983).

[14]I. Kelson, Nucl. Phys. **89**, 387 (1966); M. H. Macfarlane and A. P. Shukla, Phys. Lett. **35B**, 11 (1971).

[15]Particle Data Group, Phys. Lett. **111B**, 1 (1982).

[16]R. E. Cutkosky, C. P. Forsyth, R. E. Hendrick, and R. L. Kelly, Phys. Rev. D **20**, 2839 (1980).

[17]H. Høgaasen and J. M. Richard [Phys. Lett. **124B**, 520 (1983)] point out that orbital excitations in baryons with negative parity always come at a lower energy than states with positive parity for any general interquark confining potential.